

## THERMODYNAMIC MODELING OF THE Fe–Zn SYSTEM USING EXPONENTIAL TEMPERATURE DEPENDENCE FOR THE EXCESS GIBBS ENERGY

Y. Tang, X. Yuan, Y. Du<sup>#</sup> and W. Xiong

State Key Laboratory of Powder Metallurgy, Central South University,  
Changsha, Hunan 410083, P.R. China

*(Received 23 January 2011; accepted 20 February 2011)*

### Abstract

The Fe–Zn binary system was re-modeled using exponential equation  $L_i = h_i \cdot \exp\left(-\frac{T}{\tau_i}\right)$  ( $i = 0, 1, 2, \dots$ ) to describe the excess Gibbs energy of the solution phases and intermetallic compounds with large homogeneities. A self-consistent set of thermodynamic parameters is obtained and the calculated phase diagrams and thermodynamic properties using the exponential equation agree well with the experimental data. Compared with previous assessments using the linear equation ( $L_i = h_i - s_i \cdot T$ ) to describe the interaction parameters, the artificial miscibility gap at high temperatures was removed. In addition, the calculated thermodynamic properties of the liquid phase were more reasonable than those resulting from all the previous calculations. The present calculations yield noticeable improvements to the previous calculations.

*Keywords: Fe–Zn system; Miscibility gap; Excess Gibbs energy; Thermodynamic modelling.*

### 1. Introduction

The phase diagram is an essential tool for material development and processing design [1–3]. In the CALPHAD procedure the interaction parameter of the excess Gibbs energy is often described as linear functions

of temperature ( $L_i = h_i - T \cdot s_i$  ( $i = 0, 1, 2, \dots$ )). In some cases, an inverted artificial miscibility gap may appear at high temperatures. The problem could be solved by artificially adding some thermodynamic constraints during the optimization procedure [4]. However, a more general method is to

<sup>#</sup> Corresponding author: yongducalphad@gmail.com

introduce the exponential equation  $(L_i = h_i \cdot \exp\left(-\frac{T}{\tau_i}\right) (i=0,1,2,\dots))$ , which is suggested by Kaptay in 2004 [5], to describe the excess Gibbs energy for the solution phase. This exponential equation has been applied to the assessments of several binary systems [6–12]. These results [6–12] support the practicability of this equation.

Applying this equation to the complex Fe–Zn system to further check its practicability and obtain a self-consistent set of thermodynamic parameters are of interest due to the following reasons. Firstly, the Fe–Zn binary system is very important in the industry, especially for the galvanizing process, which requires the accurate phase

diagram. Secondly, the previous descriptions of the Fe–Zn system [13, 14] shows an artificial miscibility gap above 1529 and 1616 °C, respectively, as presented in Fig. 1. These artefacts indicate that the thermodynamic properties of liquid phase at high temperatures are not reliable physically. Thirdly, the calculated enthalpies of mixing for the liquid phase at high temperatures using all of the previous parameters [13–15] change the sign in Zn-rich side, as shown in Fig. 2. Such a behaviour is of questionable physical meaning.

In the present work, the Fe–Zn system was reassessed using the exponential equation to describe the excess Gibbs energies of all the phases including intermetallic compounds with large

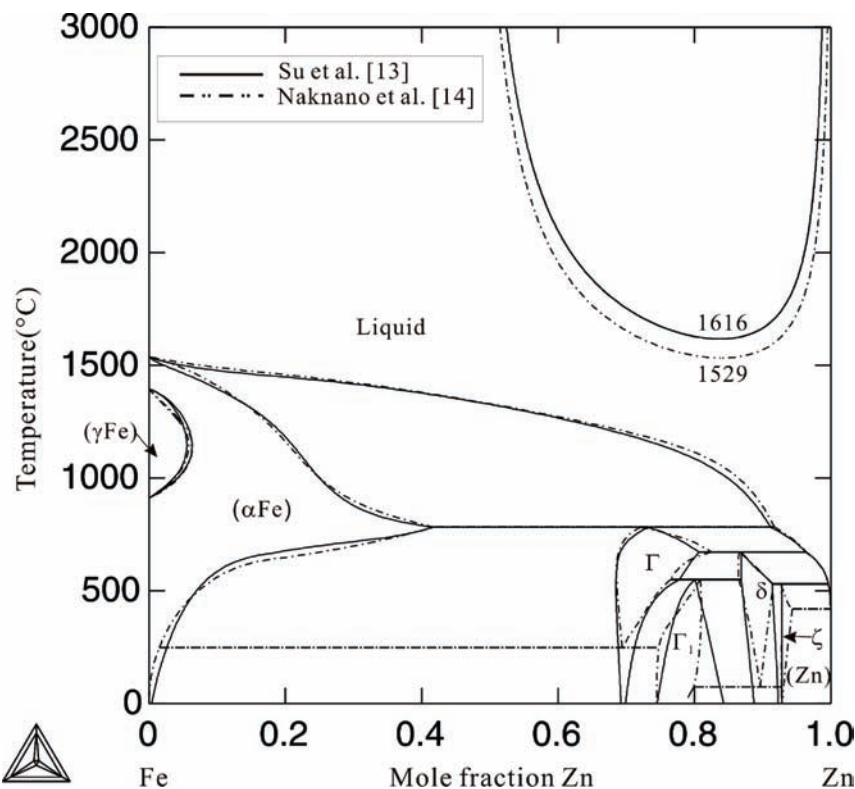


Fig. 1 Calculated Fe–Zn phase diagrams according to the previous assessment [13, 14]. The artificial miscibility gap exists above 1529 °C or 1616 °C.

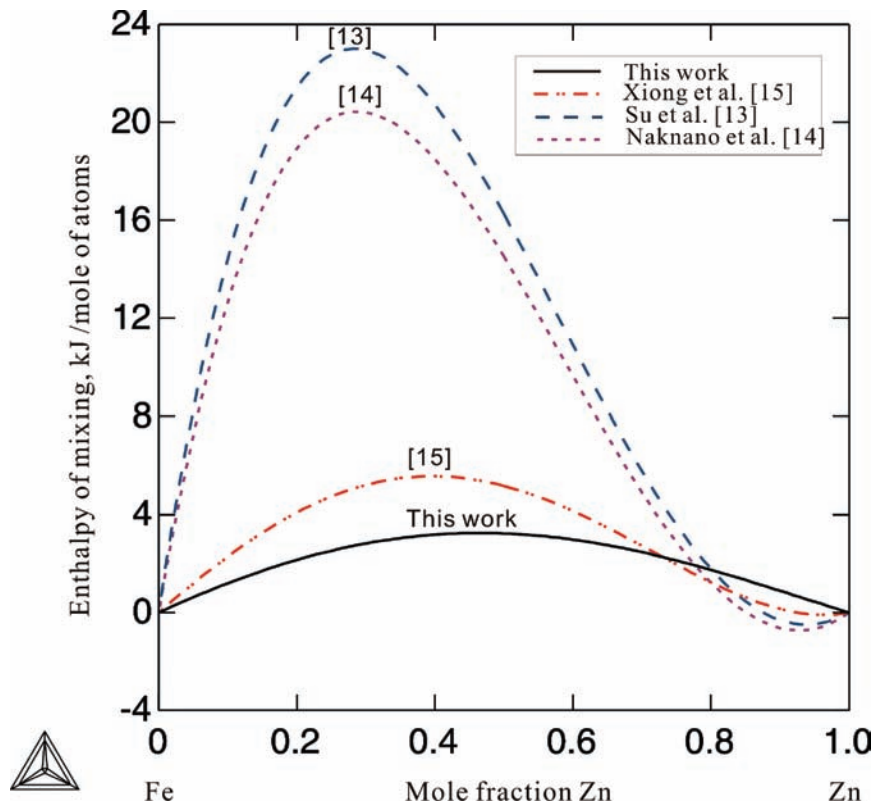


Fig. 2 Calculated enthalpies of mixing in the liquid phase at 2500 °C according to the present and previous calculations [13–15].

homogeneities. An attempt is made to obtain a set of self-consistent exponential parameters and remove the artificial miscibility gap at high temperature without applying any thermodynamic constraints during optimization procedure.

## 2. Thermodynamic model

The Fe–Zn system contains four solution phases (liquid, ( $\gamma$ Fe), (Zn), and ( $\alpha$ Fe)) and four intermetallic compounds ( $\Gamma$ ,  $\Gamma_1$ ,  $\delta$  and  $\zeta$ ). The experimental data on the phase diagram and thermodynamic properties of the Fe–Zn system were critically reviewed [13–15]. All the experimental data used in the present assessment are the same as those utilized by

Xiong et al. [15]. These data [19–35] are summarized in Table 1.

### 2.1 Pure elements

The Gibbs energy function  ${}^0G_i^\varphi(T) = G_i^\varphi(T) - H_i^{\text{SER}}$  for the element  $i$  ( $i = \text{Fe, Zn}$ ) in the  $\varphi$  phase is described by the following equation:

$${}^0G_i^\varphi(T) = a + b \cdot T + c \cdot T \cdot \ln(T) + d \cdot T^2 + e \cdot T^3 + f \cdot T^{-1} + g \cdot T^7 + h \cdot T^{-9} \quad \dots(1)$$

where  $H_i^{\text{SER}}$  is the molar enthalpy of the stable element reference at 298.15 K and 1 bar, and  $T$  is the absolute temperature. In the present work, the Gibbs energy for Fe and Zn are from the SGTE compilation by Dinsdale [16].

Table 1 Summary of the experimental data used in the present assessment

Experiment data	Method	Reference
liquidus in the Zn rich range, invarint reactions	XRD, TA	Schramm [19, 20]
liquidus in the whole range, $\gamma$ -loop and Zn solubility in ( $\alpha$ -Fe)	XRD	Budurov et al. [21]
$\gamma$ -loop boundary	Microprobe analysis	Kirchner et al. [22]
$\Gamma, \Gamma_1$ , and $\delta$ phases boundary	XRD, EPMA	Bastin et al. [23, 24]
invarint reactions	DTA, EDX, XRD	Gellings et al. [25]
Zn solubility in ( $\alpha$ -Fe)	Microscopy, XRD	Speich et al. [26]
Zn solubility in ( $\alpha$ -Fe)	Microscopy, HTXRD	Stadelmaier and Bridgers [27]
Activity of Zn	Transportation technique	Tomita et al. [28]
Activity of Zn	KEVPM	Cigan [29]
$\Delta G_f$	KEVPM	Gellings et al. [30]
Activity of Zn	Isopiestic method	Wriedt and Aarjts [31]
Activity of Zn	CA, KEVPM	Mita et al. [35]

<sup>a</sup> XRD= X-ray diffraction; EPMA= Electron probe microanalysis; TA = Thermal analysis; HTXRD=High-temperature X-ray diffraction; DTA=differential thermal analysis; EDX=Energy dispersive X-ray spectroscopy; CA=Chemical analysis; KEVPM=Knudsen effusion vapor pressure measurement.

## 2.2 Solution phases

The liquid, ( $\gamma$ Fe), (Zn), and ( $\alpha$ Fe) solution phases are described by Redlich–Kister polynomial [17], and the Gibbs energy of  $\varphi$  ( $\varphi$  = liquid or ( $\gamma$ Fe) or (Zn) or ( $\alpha$ Fe) ) is expressed as follows:

$$\begin{aligned}
 {}^0G_m^\varphi = & x_{\text{Fe}} \cdot {}^0G_{\text{Fe}} + x_{\text{Zn}} \cdot {}^0G_{\text{Zn}} + R \cdot T \cdot (x_{\text{Fe}} \cdot \\
 & \cdot \ln x_{\text{Fe}} + x_{\text{Zn}} \cdot \ln x_{\text{Zn}}) + x_{\text{Fe}} \cdot x_{\text{Zn}} \cdot \\
 & \cdot \sum_{v=0}^n {}^vL \cdot (x_{\text{Fe}} - x_{\text{Zn}})^v \quad \dots(2)
 \end{aligned}$$

where  $R$  is the gas constant, and  $x_i$  is the mole fraction of  $i$  ( $i$ =Fe or Zn). The parameter  $L$  in the last term is the interaction energy between the elements. In the present work,  $L$  is expressed by an exponential equation [5]:

$${}^vL_{\text{exp}} = h_v \cdot \exp\left(-\frac{T}{\tau_v}\right) \quad \dots(3)$$

The parameters of  $h_v$  and  $\tau_v$  are to be evaluated from the experimental phase diagram and/or thermodynamic data.

## 2.3 Intermetallic compounds with large homogeneities

The thermodynamic models for the four compounds ( $\Gamma$ ,  $\Gamma_1$ ,  $\delta$  and  $\zeta$ ) in the Fe - Zn system were well established by Nakano et al. [14]. Thus, the sublattice models used in the present assessment are the same as those in Nakano et al. [14] and shown in Table 2. The Gibbs energy per mole-formula, taking  $\zeta$ , the phase ( $(\text{Fe}, \text{Va})_{0.072}(\text{Zn})_{0.856}(\text{Zn}, \text{Va})_{0.072}$ ) for example, is expressed as:

Table 2 Summary of the evaluated thermodynamic parameters in the Fe–Zn system\*.

Phase	Model	Optimized exponential parameters
Liquid	$(Fe, Zn)_1$	${}^0L^{liq} = 125613.74 \cdot \exp(-1.38979 \cdot 10^{-3} \cdot T)$ ${}^1L^{liq} = 189615.062 \cdot \exp(-2.3496 \cdot 10^{-3} \cdot T)$ ${}^2L^{liq} = -2137.539$
( $\gamma$ Fe)	$(Fe, Zn)_1(Va)_1$	${}^0L^{fcc} = 13851.26 \cdot \exp(-3.1662 \cdot 10^{-4} \cdot T)$ ${}^1L^{fcc} = -1.672.205$
( $\alpha$ Fe)	$(Fe, Zn)_1(Va)_3$	${}^0L^{bcc} = 8332.86364$ ${}^1L^{bcc} = 5949.390 \cdot \exp(-4.983 \cdot 10^{-4} \cdot T)$ ${}^2L^{bcc} = -4833.892$
(Zn)	$(Fe, Zn)_1(Va)_{0.5}$	${}^0L^{hcp} = 23601.6208$
$\Gamma_1$	$(Fe)_{0.137}(Fe, Zn)_{0.118}(Zn)_{0.745}$	${}^0G_{Fe:Fe:Zn}^{\Gamma_1} = 0.255 \cdot {}^0G_{Fe}^{fcc} + 0.745 \cdot {}^0G_{Zn}^{hcp} - 7601.816 + 4.7440 \cdot T$ ${}^0G_{Fe:Zn:Zn}^{\Gamma_1} = 0.137 \cdot {}^0G_{Fe}^{fcc} + 0.863 \cdot {}^0G_{Zn}^{hcp} - 2908.620$ ${}^0L_{Fe:Fe:Zn:Zn}^{\Gamma_1} = -18730.792 \cdot \exp(-3.91966 \cdot 10^{-3} \cdot T)$
$\delta$	$(Fe)_{0.058}(Fe, Zn)_{0.18}(Zn)_{0.525}(Zn)_{0.237}$	${}^0G_{Fe:Fe:Zn:Zn}^{\delta} = 0.238 \cdot {}^0G_{Fe}^{fcc} + 0.762 \cdot {}^0G_{Zn}^{hcp} - 2569.236$ ${}^0G_{Fe:Zn:Zn:Zn}^{\delta} = 0.058 \cdot {}^0G_{Fe}^{fcc} + 0.942 \cdot {}^0G_{Zn}^{hcp} - 2169.039$ ${}^0L_{Fe:Fe:Zn:Zn:Zn}^{\delta} = -9101.82 \cdot \exp(-1.810788 \cdot 10^{-3} \cdot T)$
$\Gamma$	$(Fe, Zn)_{0.154}(Fe, Zn)_{0.154}(Fe, Zn)_{0.231}(Zn)_{0.461}$	${}^0G_{Fe:Fe:Fe:Zn}^{\Gamma} = 0.539 \cdot {}^0G_{Fe}^{fcc} + 0.461 \cdot {}^0G_{Zn}^{hcp}$ ${}^0G_{Zn:Fe:Fe:Zn}^{\Gamma} = 0.385 \cdot {}^0G_{Fe}^{fcc} + 0.615 \cdot {}^0G_{Zn}^{hcp}$ ${}^0G_{Fe:Zn:Fe:Zn}^{\Gamma} = 0.385 \cdot {}^0G_{Fe}^{fcc} + 0.615 \cdot {}^0G_{Zn}^{hcp} - 6151.60 + 3.9918 \cdot T$ ${}^0G_{Zn:Zn:Fe:Zn}^{\Gamma} = 0.231 \cdot {}^0G_{Fe}^{fcc} + 0.769 \cdot {}^0G_{Zn}^{hcp} + 6316.923$ ${}^0G_{Fe:Fe:Zn:Zn}^{\Gamma} = 0.308 \cdot {}^0G_{Fe}^{fcc} + 0.692 \cdot {}^0G_{Zn}^{hcp}$ ${}^0G_{Zn:Fe:Zn:Zn}^{\Gamma} = 0.154 \cdot {}^0G_{Fe}^{fcc} + 0.846 \cdot {}^0G_{Zn}^{hcp}$ ${}^0G_{Fe:Zn:Zn:Zn}^{\Gamma} = 0.154 \cdot {}^0G_{Fe}^{fcc} + 0.846 \cdot {}^0G_{Zn}^{hcp} - 2646.02639$ ${}^0G_{Zn:Zn:Zn:Zn}^{\Gamma} = {}^0G_{Zn}^{hcp} + 4830.0 - 6.91322 \cdot T$ ${}^0L_{Fe:Zn:Fe:Zn:Zn}^{\Gamma} = -23177.2116 \cdot \exp(-2.90583 \cdot 10^{-3} \cdot T)$
$\zeta$	$(Fe, Va)_{0.072}(Zn)_{0.856}(Zn, Va)_{0.072}$	${}^0G_{Fe:Zn:Va}^{\zeta} = 0.072 \cdot {}^0G_{Fe}^{fcc} + 0.856 \cdot {}^0G_{Zn}^{hcp} + 983.46$ ${}^0G_{Va:Zn:Va}^{\zeta} = 0.856 \cdot {}^0G_{Zn}^{hcp} + 81.00$ ${}^0G_{Fe:Zn:Zn}^{\zeta} = 0.072 \cdot {}^0G_{Fe}^{fcc} + 0.928 \cdot {}^0G_{Zn}^{hcp} - 2720.00$ ${}^0G_{Va:Zn:Zn}^{\zeta} = 0.928 \cdot {}^0G_{Zn}^{hcp} + 764.75$

\* In J/(mol-atoms); Temperature(T) in Kelvin.

$$\begin{aligned}
{}^0G_m^{\zeta} = & y'_{Fe} y'''_{Zn} {}^0G_{Fe:Zn:Zn} + y'_{Fe} y'''_{Va} {}^0G_{Fe:Zn:Va} + (y'''_{Zn} \ln y'''_{Zn} + y'''_{Va} \ln y'''_{Va})] + {}^{ex}G_m \quad \dots(4) \\
& + y'_{Va} y'''_{Zn} {}^0G_{Va:Zn:Zn} + y'_{Va} y'''_{Va} {}^0G_{Va:Zn:Va} \\
& + 0.072 \cdot RT \cdot [(y'_{Fe} \ln y'_{Fe} + y'_{Va} \ln y'_{Va}) + (y'''_{Zn} \ln y'''_{Zn}
\end{aligned}$$

in which  $y'_{Fe}$  and  $y'_{Va}$  are the site fractions of Fe and vacancy in the first sublattice, respectively, and  $y'''_{Zn}$  and  $y'''_{Va}$  are the site

fractions of Zn and vacancy in the third sublattice, respectively. In the present work, the term  ${}^{\text{ex}}G_m$  reads:

$$\begin{aligned} {}^{\text{ex}}G_m = & y'_{\text{Fe}} y'_{\text{Va}} y''_{\text{Zn}} \sum_{v=0}^n v L_{\text{Fe,Va:Zn:Zn}} \cdot (y'_{\text{Fe}} - \\ & y'_{\text{Va}})^v + y'_{\text{Fe}} y'_{\text{Va}} y''_{\text{Va}} \sum_{v=0}^n v L_{\text{Fe,Va:Zn:Va}} \cdot (y'_{\text{Fe}} - \\ & y'_{\text{Va}})^v + y'_{\text{Fe}} y''_{\text{Zn}} y''_{\text{Va}} \sum_{v=0}^n v L_{\text{Fe:Zn:Zn,Va}} \cdot (y''_{\text{Zn}} - \\ & y''_{\text{Va}})^v + y'_{\text{Va}} y''_{\text{Zn}} y''_{\text{Va}} \sum_{v=0}^n v L_{\text{Va:Zn:Zn,Va}} \cdot (y''_{\text{Zn}} - \\ & y''_{\text{Va}})^v \end{aligned} \quad \dots(5)$$

in which the  $L$  parameters represent the interaction energies within each sublattice. They are also expressed by an exponential equation Eq.(3). The Gibbs energies of  $\Gamma$ ,  $\Gamma_1$ ,  $\delta$  phases are represented with the analogous equation.

### 3. Results and discussion

The optimization was carried out by using the PARROT module in the Thermo-Calc software [18], which works by minimizing the square sum of the differences between the measured and calculated values. In the assessment procedure, each selected piece of experimental information was given a certain weight. The weights were changed systematically during the assessment until most of the selected experimental information was reproduced within the expected uncertainty limits.

In the first step of the present assessment, only the thermodynamic data including the activity of Zn and Gibbs energy of formation were considered to determine the parameters  $h_v$  in Eq.(3) for solution phases and the intermetallic compounds. Secondly, parameter  $\tau_v$  can be adjusted by using all the invariant

reactions to describe the general feature of the phase diagram. Thirdly, the experimental data on liquidus and solubility of Zn in ( $\alpha$ Fe) were utilized to refine the above preliminary optimization. Finally, all of the selected experimental data were used simultaneously in order to get a self-consistent set of thermodynamic parameters. The finally obtained parameters are listed in Table 2.

Using the presently obtained parameters, the calculated Fe–Zn phase diagram along with the experimental data [19–25, 28] is shown in Fig. 3. The calculated phase boundaries agree well with the experimental data. The calculated compositions and temperatures for the invariant reactions along with the experimental data [25] are listed in Table 3. It shows that the deviations between the calculation and experiment are very small. Besides, the miscibility gap at high temperatures, as shown in Fig. 1, was removed in the present work. This is an addition confirmation on the reliability of the exponential equation.

The activities of Zn at 700, 750, 800 and 1585 °C are shown in Fig. 4(a–d). Within the claimed experimental uncertainties, the calculation reproduces the experimental data [28, 31–33] reasonably. Although the experimental data on the activity of Zn at 1585 °C [32, 33] were not used in this optimization, the computed values are in consistent with the experimental results of Dimov et al. [33]. Such a good agreement further verifies the soundness of the present modeling. The calculated activity in solid phase at 400 °C together with experimental results [34, 35] is shown in Fig. 5. The calculated and experimental values show a good agreement with each other.

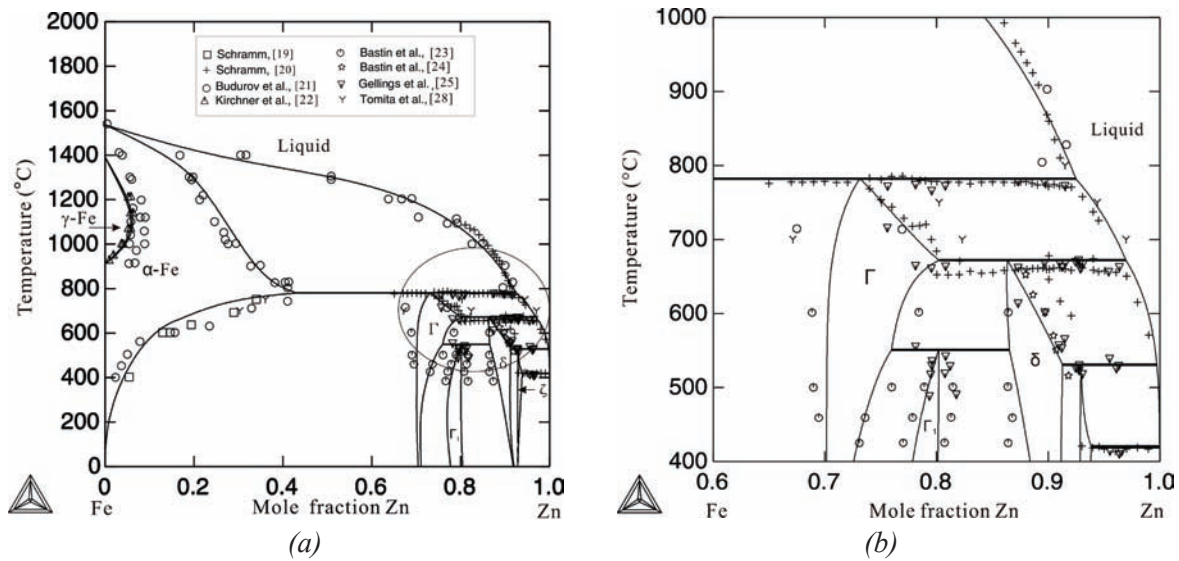


Fig. 3 The presently calculated phase diagram along with the experimental data [19–25, 28]. (a) from Fe to Zn, (b) magnified region in Fig.3 (a).

In order to check the thermodynamic properties of liquid at high temperatures, the calculated enthalpies of mixing in liquid phase at 2500 °C from various sources are presented in Fig. 2. All the previous calculations [13–15] indicate negative values in the Zn-rich side and positive values in the other composition region. Such

a behaviour associated with the previous calculations [13–15] was unusual in view of the general belief that one particular system usually shows either positive or negative enthalpy of mixing for the liquid over the whole composition range. The present calculation yields positive values over the whole composition range, indicating a

Table 3 Comparison of the invariant reactions from different sources.

Reaction	Composition (at.%Zn)	T(°C)	Type	Reference
$(\alpha\text{Fe})+\text{L} \leftrightarrow \Gamma$	43.20 92.49 73.16	782.0	calculation, exponential equation	This work
	42.30 92.00 72.60	782.0	calculation, linear equation	[15]
	42.00 92.00 72.00	782.0	experiment	[25]
$\text{L}+\Gamma \leftrightarrow \delta$	80.22 96.97 86.36	672.0	calculation, exponential equation	This work
	82.70 97.30 85.60	668.0	calculation, linear equation	[15]
	82.50 96.50 86.50	672.0	experiment	[25]
$\Gamma+\delta \leftrightarrow \Gamma_1$	75.97 86.54 80.20	550.7	calculation, exponential equation	This work
	76.80 85.60 81.00	550.0	calculation, linear equation	[15]
	76.50 86.50 81.00	550.0	experiment	[25]
$\delta+\text{L} \leftrightarrow \zeta$	91.30 99.74 92.94	530.7	calculation, exponential equation	This work
	91.40 99.85 93.00	526.0	calculation, linear equation	[15]
	92.00 99.50 92.70	530.0	experiment	[25]
$\text{L}+\zeta \leftrightarrow (\text{Zn})$	99.988 93.88 99.9886	419.5	calculation, exponential equation	This work
	99.998 93.90 99.9886	419.5	calculation, linear equation	[15]
	99.989 94.00 100.00	419.4	experiment	[25]

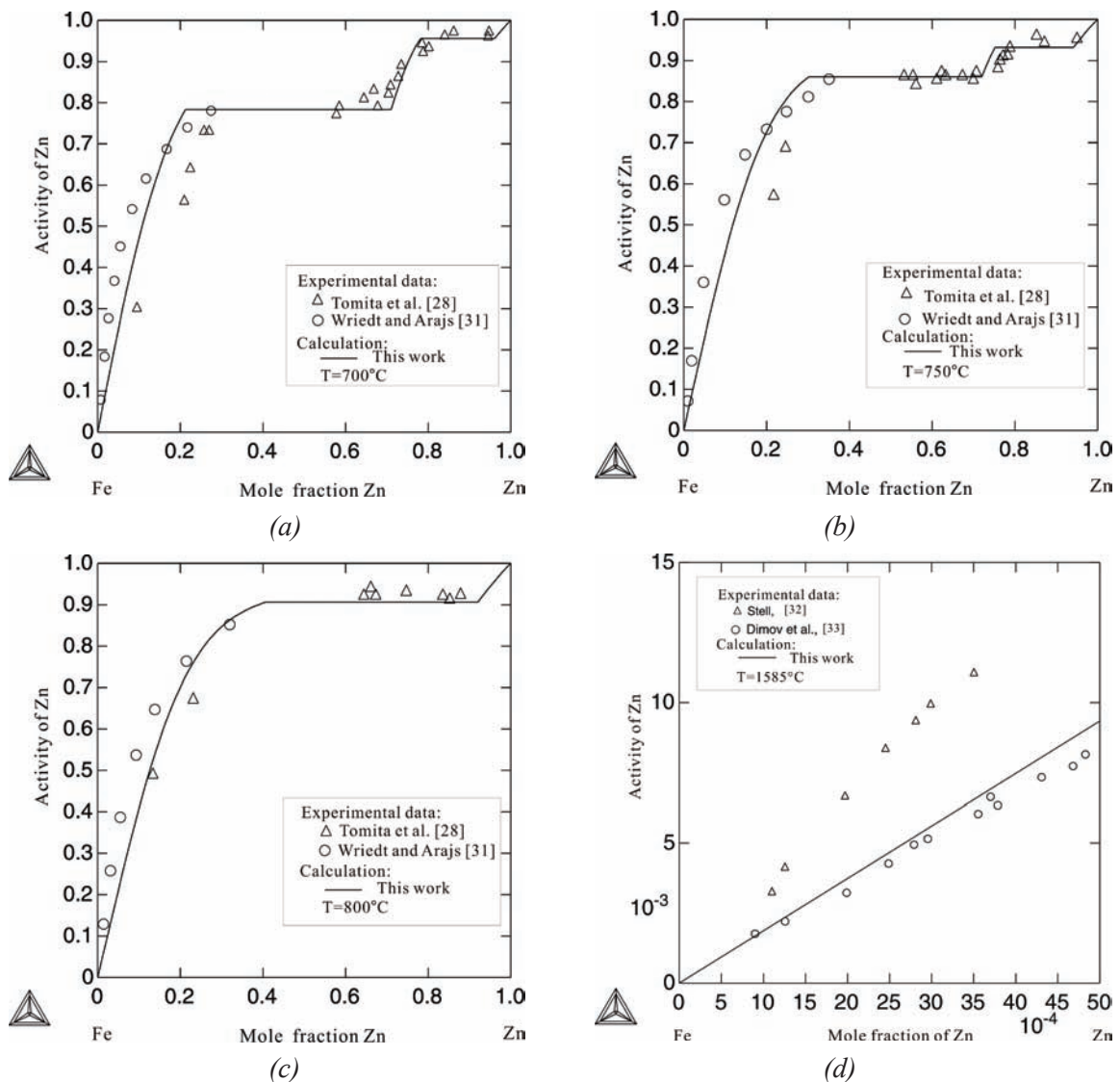


Fig. 4 Calculated activity of Zn with the experimental data [28, 31–33] (a) 700 °C, (b) 750 °C, (c) 800 °C and (d) 1585 °C. The reference states are liquid Fe and Zn.

physically sound modeling for the thermodynamic properties at high temperatures. Using the presently optimized parameters, the calculated enthalpies of mixing at different temperatures 1600, 2500 and 3500 °C are presented in Fig. 6. It shows that the enthalpies of mixing become smaller when the temperature increases. Such a behavior is consistent with the general belief that the liquid approaches to the ideal

solution at very high temperature. However, when using the linear function to describe the excess Gibbs energy, the calculated enthalpies of mixing in the liquid phase are constant at different temperatures [9]. The linear function failed to realize the ideal solution feature for the liquid at very high temperatures.

The present work shows that the exponential equation for the excess Gibbs



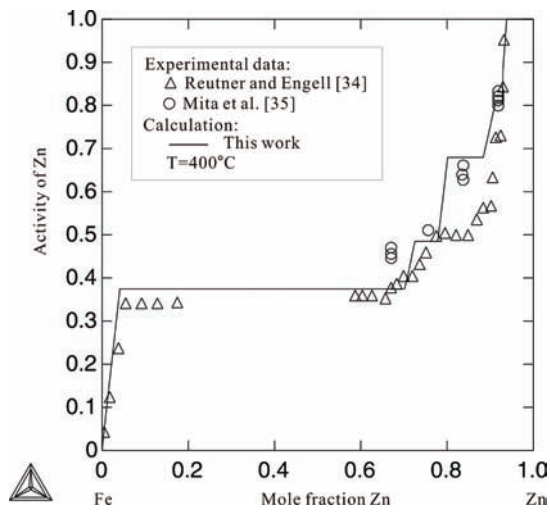


Fig. 5 Calculated activity of Zn using the present parameters together with the experimental data [34, 35] at 400 °C. The reference state is hcp-Zn.

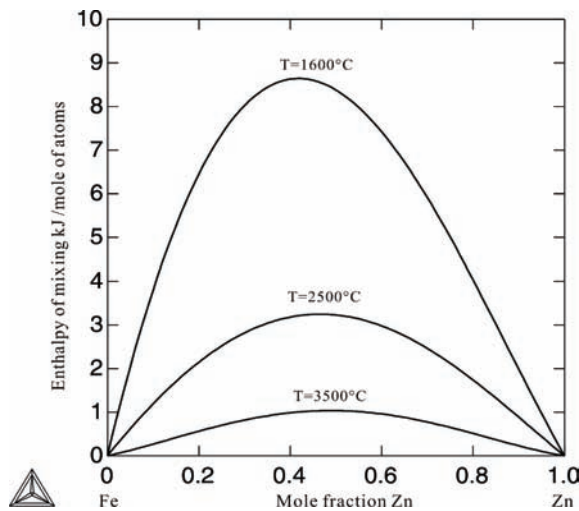


Fig. 6 Predicted enthalpy of mixing in the liquid phase at different temperatures. The reference state is liquid Fe and Zn.

energy is very efficient to remove the artificial miscibility gap at high temperature. Besides, the calculated thermodynamic properties using exponential equation is more reasonable than those due to the linear equation. It is recommended that the binary systems, which show artificial miscibility

gap in the literature, should be checked and reassessed using the exponential equation.

#### 4. Conclusion

The exponential equation was successfully used to describe the excess Gibbs energy of both liquid and solid phases in the Fe-Zn system. A set of self-consistent thermodynamic parameters of the Fe-Zn system was obtained. The calculated phase diagrams and thermodynamic properties using the obtained exponential parameters are in a good agreement with the experiments. Noticeable improvements have been made, in comparison with previous assessments.

The artificial miscibility gap in the liquid phase at high temperatures was removed automatically using the exponential equation without applying any thermodynamic constraints. Such a miscibility gap may appear when the R-K linear polynomial was used without adding the constraints during the thermodynamic optimization.

#### Acknowledgements

The financial support from the Creative Research Group of National Natural Science Foundation of China (Grant No. 51021063), National Basic Research Program of China (Grant No. 2011CB610401) and the key program of the National Natural Science Foundation of China (Grant No. 50831007) is acknowledged.

#### References

- [1] Y. Du, J. Wang, Y.F. Ouyang, L.J. Zhang,

- Z.H. Yuan, S.H. Liu, P. Nash, J. Min. Metall. Sect. B., 46(1) (2010) 1.
- [2] Y. Du, X. Yuan, W. Sun, B. Hu, J. Min. Metall. Sect. B., 45(1) (2009) 89.
- [3] A. Kostov, B. Friedrich, D. Živković, J. Min. Metall. Sect. B., 44 (1) (2008) 49.
- [4] P. S. Wang, L. C. Zhou, Y. Du, H. H. Xu, S. H. Liu, L. Chen, Y.F. Ouyang, J. Alloys Comp., 509 (2011) 2679.
- [5] G. Kaptay, CALPHAD, 28 (2004) 115.
- [6] H. Ran, Z. Du, C. Guo, C. Li, J. Alloys Comp., 464(2008) 127.
- [7] Y. Gao, C. Guo, C. Li, S. Cui, Z. Du, J. Alloys Comp., 497 (2009) 148.
- [8] M. Li, C. Guo, C. Li, Z. Du, J. Alloys Comp., 481 (2009) 283.
- [9] X. Yuan, W. Sun, Y. Du, D. Zhao, H. Yang, CALPHAD, 33 (2009) 673.
- [10] C. Y. Zhan, W. Wang, Z. L. Tang, Z. R. Nie, Mater. Sci. Forum, 610–613 (2009) 674.
- [11] R. Arroyave, Z. K. Liu, CALPHAD, 30 (2006) 1.
- [12] C. Guo, C. Li, Z. Du, J. Alloys Comp., 492 (2009) 122.
- [13] X. Su, N. Y. Tang, J. M. Toguri, J. Alloys Comp., 325 (2001) 129.
- [14] J. Naknana, D. V. Malakhov, G. R. Purdy, CALPHAD, 29 (2005) 276.
- [15] W. Xiong, Y. Kong, Y. Du, Z. K. Liu, CALPHAD, 33 (2009) 433.
- [16] A. T. Dinsdale, CALPHAD, 15 (1991) 317.
- [17] O. Redlich, A. T. Kister, Ind. Eng. Chem., 40(1948) 345.
- [18] B. Sundman, B. Jansson, J. O. Andersson, CALPHAD, 9 (1985) 153.
- [19] J. Schramm, Z. Metallkd., 28 (1936) 203.
- [20] J. Schramm, Z. Metallkd., 30 (1938) 122.
- [21] S. Budurov, P. Kovatchev, N. Stojčev, Z. Kamenova, Z. Metallkd., 63 (1972) 348.
- [22] G. Kirchner, H. Harvig, K. R. Moquist, M. Hillert, Arch. Eisenhüttenwes., 44 (1973) 227.
- [23] G. F. Bastin, F. J. J. Van Loo, G. D. Rieck, Z. Metallkd., 68 (1974) 657.
- [24] G. F. Bastin, F. J. J. Van Loo, G. D. Rieck, Z. Metallkd., 68 (1977) 359.
- [25] P. J. Gellings, G. Gierman, D. Koster, J. Kuit, Z. Metallkd., 71 (1980) 150.
- [26] G. R. Speich, L. Swell, H. A. Wriedt, T. Am. I. Min. Met. Petrol. Eng., 230 (1964) 939.
- [27] H. H. Stadelmaier, R. K. Bridgers, Metallurgia, 15 (1961) 761.
- [28] M. Tomita, T. Azakami, L. M. Timberg, J. M. Toguri, Trans. Jpn. Inst. Met., 22 (10) (1981) 717.
- [29] J. M. Cigan, Thesis for the Degree of Doctor of Philosophy, Carnegie Institute of Technology, 1960.
- [30] P. J. Gellings, G. Gierman, D. Koster, J. Kuit, Z. Metallkd., 71 (1980) 70.
- [31] H. A. Wriedt, S. Arajs, Phys. Status Solidi, 16 (1966) 475.
- [32] A. Stell, Tablizi dawlenia Parov individualnich westestv, Gossudarstvenoe izdatelstwo innostranoi literatury, Moskau, 1949.
- [33] I. Dimov, D. Nenov, N. Gidikova, A. Mozeva, Arch. Eisenhüttenwes., 48 (1977) 209.
- [34] P. Reutner, H. J. Engell, Arch. Eisenhüttenwes., 51 (1980) 457.
- [35] K. Mita, S. Yamaguchi, M. Maeda, Metall. Mater. Trans. B, 35 (2004) 487.